The PARIS Concept: An Experimental Demonstration of Sea Surface Altimetry Using GPS Reflected Signals

Manuel Martín-Neira, Marco Caparrini, J. Font-Rossello, Stephane Lannelongue, and Circe Serra Vallmitjana

***Abstract*—This paper presents the passive reflectometry and interferometry system (PARIS) concept and how it originated in the European Space Agency (ESA), Noordwijk, The Netherlands, in 1993 as a novel method to perform mesoscale ocean altimetry. The PARIS concept uses signals of opportunity such as the signals from the global navigation satellite systems (GNSS), which are reflected off the ocean surface to perform mesoscale ocean altimetry. Essentially, the relative delay between the direct and the reflected signals received from a Low Earth Orbit satellite provides information about sea surface height.**

The paper describes an original experiment on sea surface altimetry using GPS-reflected signals. The objective of the experiment was to demonstrate the potential of the PARIS concept. This experiment is the first one ever published on performing sea surface height estimations using reflected navigation signals in a controlled environment. The key result of the experiment is the demonstration of a root mean squared (RMS) height accuracy within 5 s of 1% of the used code chip (3 m for C/A code). Direct extrapolation of this experimental result to the 10-times higher chip rate P-code signal allows us to predict a height error of 30 cm in 5 s, provided adequate models are used to take into account systematic effects.

The paper ends presenting the potential of the PARIS concept for long term ocean altimetric observations in view of the current trends of the GNSS systems.

***Index Terms*—Global navigation satellite systems (GNSSs) reflected signals, mesoscale ocean, ocean altimetry.**

I. Introduction

BACK in June 1990, right at the beginning of the decade when multiple nadir-looking radar altimeters (e.g., ERS-1/2, the U.S. Navy's SALT, the U.S.-French TOPEX Poseidon, and the ESA Polar Platform RA-2) would be flying simultaneously for the first time ever, the European Space Agency (ESA) sponsored the *Consultative Meeting on Imaging Altimeter Requirements and Techniques* at the Mullard Space Science Laboratory, University College, London, U.K. One of the technical conclusions was that "A constellation of five pulse-limited altimeter satellites would solve the temporal-spatial sampling requirements for ocean mesoscale studies and would improve significantly the capability for other applications (e.g., wave–wind, ocean–sea ice interactions, etc.)" [1]. Based on the recommendations from this consultative meeting, ESA initiated the study of a constellation of pulse-limited nadir-looking radar altimeters. This study finished in 1992 concluding that a constellation of eight satellites was needed to achieve a goal sampling requirement for mesoscale ocean observations with a seven-day revisit time and a 50-km spatial resolution [2].

In an attempt to simplify the constellation of eight nadir-looking radar altimeters, while keeping the sampling requirements for mesoscale ocean, Martin-Neira proposed, for the first time, the use of the GPS signals reflected off the ocean surface as ranging signals. Many reflections could be simultaneously received (as many as visible GPS satellites) and thus, there was no need anymore for a constellation of satellites. Just one would achieve high temporal and spatial sampling. The system was pulse-limited, and echo waveforms could be generated, from which information about sea surface height, wind, and significant wave height could be derived through model fitting as in nadir-looking altimetry. The general concept of using of signals of opportunity for ocean observations, called "passive reflectometry and interferometry system," (PARIS), was submitted to the patent board of ESA on August 3, 1993 (first filing on November 5, 1993 [3]) and was first published in the December 1993 issue of the *ESA Journal* [4].

The *ESA Journal* article describes PARIS and its fundamentals (as the computation of the reflection points, iso-range and iso-doppler contours, SNR, and performance) and the basic instrument configuration for its implementation on a low Earth orbit satellite. The predicted accuracy in sea surface height using the GPS P-code was 0.7 m in 0.8 s and the spatial resolution better than 30 km. Since the signal to noise ratio from low Earth orbit was estimated to be low (in particular when using the P-code) the system required a large (more than 10 m^2) antenna.

This first study was followed by the development of a bistatic model of the ocean scattering under ESA contract to La Sapienza University, Rome, Italy [5]. This work extended the classical Brown model used in nadir-looking pulse-limited altimeters to the bistatic configuration, including the case of nongaussian surface statistics. In this way the measured waveform can be compared to the model to perform not only sea surface height, but also wave and wind estimations. The Rao–Cramer bounds were computed, confirming the above-mentioned expected performance.

In September 1994, Jean-Claude Auber from Dassault Electronique, France, reported the locking of a GPS receiver onboard an Alfajet aircraft onto a reflected signal during flight trials over the Atlantic [6]. This was the first experimental observation ever

Manuscript received November 9, 1999; revised April 27, 2000.

The authors are with the European Space Research and Technology Center (ESTEC), European Space Agency (ESA), Noordwijk, The Netherlands.

Publisher Item Identifier S 0196-2892(01)00347-3.

related to the PARIS concept from aircraft. The first evidence of a GPS reflection picked up from orbit was reported by Steve Lowe (JPL) in July 1998, using 4 s of "receive-only" mode data of the Radar Laboratory 2 SIR-C aboard the Shuttle [7].

II. Preliminary Theoretical Considerations

A. Required Accuracy for Mesoscale Ocean Altimetry

It has been recognized for a decade now that the ability to perform precise ocean altimetry over a swath of at least some 250 km, i.e., significantly wider than with conventional altimeters, would greatly contribute to many fields of Earth science. With a single or a few pulse-limited altimeters, the temporal sampling interval must be traded against the density of subsatellite tracks. This limits the ability to study ocean mesoscale flows with a spatial scale of approximately 50–200 km (e.g.,, eddies, fronts, warm and cold rings, jets). These short scale variations tend to occur over time periods of weeks to months. Expected amplitudes for mesoscale eddies and meanders at mid- and high latitudes is in the range 5–30 cm, down to a few cm for high latitude fronts [8]. Assuming a required sensitivity equal to 20% of the signal, mesoscale ocean altimetry calls for a precision between 1 and 5 cm.

The estimated error (in approximately 1 s and 30 km spatial resolution) using GPS P-code is at present one order of magnitude too high for these applications, mainly due to the relatively narrow bandwidth of the signals [4]. There is therefore a need to improve this precision to the subdecimeter level. This can be done by massive averaging of 1 s samples at the expense of losing some temporal-spatial resolution. In the future, when the GPS satellites transmit three civilian frequencies as it is planned, an improved performance should also be expected.

In summary, precision is an issue when using reflected GPS signals for mesoscale ocean altimetry and more theoretical and experimental work must be carried out in this area. The experiment presented in this paper is just a first step.

B. Direct and Reflected Signal Equations

With reference to Fig. 1, the direct signal from a particular GPS satellite can be approximately described by

$$x_d(t) = p\left[t - r_d(t)/c - K/f_c^2\right]\ e^{-j2\pi f_c\left[t - r_d(t)/c + K/f_c^2\right]} \tag{1}$$

where

- f_c L1 carrier frequency (L1 = 1575.42 MHz);
- $p(t)$ C/A-code;
- $r_d(t)$ distance from the receiving antenna to the GPS satellite;
- K/f_c^2 accounts for the ionospheric effect.

The reflected signal from the same GPS satellite, using the Kirchhoff approximation, takes the form of an integral of delayed versions of the direct signal affected by the bistatic radar cross section

$$x_r(t) = \int F(\mathbf{P})\sqrt{\sigma(\mathbf{P})}p\left[t - r(\mathbf{P}, t)/c - K/f_c^2\right] \cdot e^{-j2\pi f_c[t - r(\mathbf{P}, t)/c + K/f_c^2]}\, dA(\mathbf{P}) \tag{2}$$

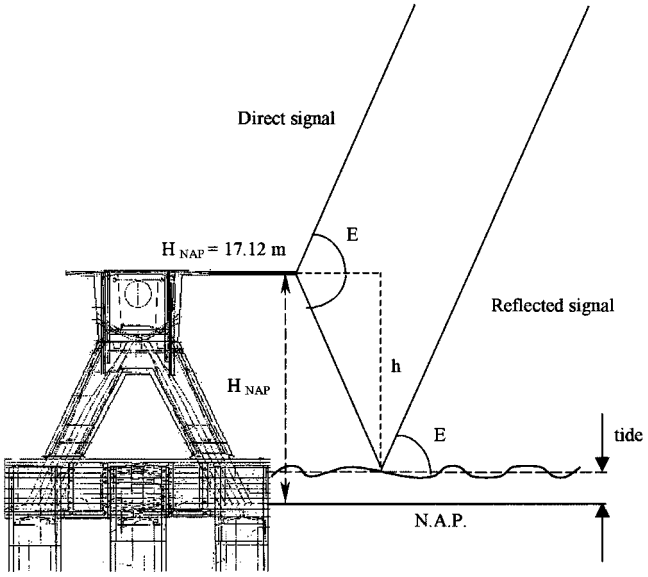

Fig. 1. Geometry of direct and reflected signals in the Zeeland Bridge experiment. The nominal height of the bridge (at the antenna location) with respect to the mean sea level in Amsterdam Harbor (Normaal Amsterdams Peil: N.A.P.) is 17.12 m.

where

- $\mathbf{P}(x, y, \varsigma)$ point on the surface defined by its coordinates in the horizontal plane (x, y) and its elevation ς;
- $F(\mathbf{P})$ voltage gain of the receiving antenna in the direction of $\mathbf{P}$;
- $\sigma(\mathbf{P})$ bistatic radar cross section per unit area;
- $r(\mathbf{P}, t)$ geometrical path length of the ray scattered from $\mathbf{P}$;
- $dA(\mathbf{P})$ small element of area centered at $\mathbf{P}$.

Since the position of $\mathbf{P}$ depends on the roughness of the surface ς, both the path length of the scattered ray and the element of area depend also on the roughness.

The basic operation to retrieve the sea surface altimetry is the cross correlation of a clean replica of the direct signal of a particular satellite and the global reflected signal

$$R_{x_d x_r}(\tau; t) \equiv \langle x_d(t) x_r^*(t - \tau)\rangle \tag{3}$$

It can be demonstrated that the echo-waveform provided by such cross-correlation function is given by [9] (see Appendix I)

$$R_{x_d\, x_r}(\tau; t) = \int F(\mathbf{P})\ \sqrt{\sigma(\mathbf{P})}\ R_p\left[\tau - r_d(\mathbf{P}, t)/c\right] \cdot \mathrm{sinc}[f_d(\mathbf{P})T] e^{-j\ 2\pi f_d(\mathbf{P})[\ t - T/2]}\, dA(\mathbf{P}) \tag{4}$$

where

- $R_p(\tau)$ auto-correlation function of the C/A code;
- $r_d(\mathbf{P}, t)$ and $f_d(\mathbf{P})$ delay and dopper frequency of the signal scattered by the area element $dA(\mathbf{P})$ with respect to the direct signal;
- T integration time used in the estimation of the cross correlation.

Fig. 2. Antenna arrangement: a RHCP 2-dBic zenith-looking and a LHCP 9-dBic nadir-looking antenna, back to back, at the tip of a 4.5 m mast over the edge of the bridge.

III. Experimental Work

Two experiments were performed on the "Zeeland Brug" (Zeeland Bridge) near Rotterdam, The Netherlands, in September 4 and 8, 1997. The goal of this experiment was to record the maximum information on direct and reflected signals in order to be able to study and compare them, in particular for sea surface altimetry.

A. Reception and Amplification

Two antennas back-to-back were used in the experiment, one for direct signals and another for reflected ones (see Fig. 2). Direct signals were received by a right-hand circular polarized (RHCP) 2-dBic gain antenna by M/A-COM. Its bandwidth is 10 MHz with a central frequency at 1575 MHz (L band). After reception, the direct signal was amplified with a low noise amplifier (LNA) of 26 dB gain and a noise figure of 2.5 dB. This reception chain was exactly the one provided in the GPSbldr2 package of GEC Plessey. The antenna and the LNA were implemented in the same module. The reflected signal was received by a passive helical antenna with 9-dBic gain and left hand circular polarization (LHCP). A Miteq LNA with a noise figure of 0.8 dB and a gain of 41.5 dB from 1.2 to 1.6 GHz was used. Both antennas were placed at the tip of a 4.5-m long mast. The RHCP antenna was zenith pointed, whereas the LHCP antenna was nadir pointed in order to receive the GPS signals reflected from the sea.

B. Sampling and File Recording

After amplification, each signal was sent to a different GPS receiver. We used for this experiment two GPS-builder kit-2 designed by GEC-Plessey. These receivers were used to carry out two tasks. The first one was to record, for all satellites in view, pseudoranges, ephemeris, integrated doppler, doppler frequencies and clock biases in rinex format files. Furthermore a slight modification in the receivers software was implemented to record signal to noise ratio as indicated by the receiver for all satellites. The second task of the GPS-builders was to complete the down-conversion from L-band to intermediate frequency in order to record the direct and the reflected signals by a sampling unit. The RF front-end of a GPS-bldr2 receiver down-converts the GPS signals from L-band to an IF center frequency of 4.309 MHz with a bandwidth of 1.9 MHz. The IF signal is not available as an output in that kind of receiver, and some modifications were needed to make this signal accessible to the sampling unit. The IF signals were sent directly to a high performance sampling card, namely, the DA500 board by Signatec, which is able to sample a signal up to 240 MHz.

In order to increase the amount of data recorded while avoiding aliasing, the IF band-limited signals (both direct and reflected) were simultaneously undersampled at 6.25 MHz and quantified with 8 bits. Samples were stored in real time in a memory board (MEM500 of Signatec) with a storage capacity of 32 Mb. Some 30 runs were completed with a duration of 2.56 s, giving a cumulative observation time of about 80 s each day, where the direct and the reflected signals were recorded simultaneously. At the end of each run, the recorded data were saved on digital tapes. Since the transfer of data into the tape took 10 min every time, the total duration of each experiment was about 4 to 5 h. During the whole duration of the experiments, the rinex files were stored in parallel.

The downlooking receiver locked onto as many satellites as the uplooking one showing the code, carrier, bit and frame locking flags on. Despite these indicators the downlooking receiver was not able to provide pseudoranges, and all we have in the rinex measurement files is carrier phase data.

IV. Data Processing

A. Preliminary Analysis

The data processing to retrieve the sea surface height focused on the measurements of the second day (Sept. 8, 1997). The GPS signals were considered suitable for the processing if their SNR was greater than a certain threshold (usually a threshold of 9 dB for the reflected signal SNR is enough to make the choice since, in these cases, the direct signal SNR is also sufficiently high). Another element to be considered in order to accept a signal for the processing was the position of the GPS satellites. "Good" satellites are those belonging to two windows in the azimuth elevation plane. The criterion to define these windows is simply to avoid all transmitter-to-receiver directions that could generate reflection phenomena on the artificial structures in the neighborhood of the antennas. First of all, the direction parallel to the bridge has been rejected. Then, all directions (in azimuth) lying on the same side of the bridge as the antenna where considered good, while the elevation was restricted to be greater than 10°. On the opposite side of the bridge, the extreme acceptable values for the GPS satellite elevation and azimuth come from geometrical considerations of obstruction from the bridge structure. In particular, the azimuth limitations arise from the angle between the bridge and the transmitter-to-receiver direction. As this angle decreases, the bridge structure can interfere with the first Fresnel zone of the electromagnetic link. Of course there is a relationship between the minimum elevation angle allowed and the possible excursion of the azimuth. All these geometrical constraints to ensure obstruction-free reflected signals resulted in a mask in the azimuth-elevation plane.

Fig. 3 shows the azimuth-elevation plane with the available (represented by a circle ○) and the actually used GPS satel-

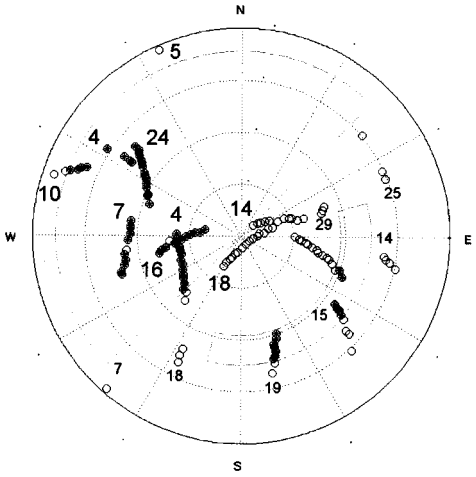

Fig. 3. Azimuth-elevation 3-h location plot of the available GPS satellites. The Zeeland Bridge orientation is from Northeast to Southwest. The antennas were on the Northwest side of the bridge. The mask to ensure obstruction-free reflected signals is shown. Good satellite locations (high SNR and unobstructed reflection) are represented by filled circles. Invalid directions (low SNR and/or obstructed reflection) are marked with empty circles.

TABLE I
LOCAL TIME OF MEASUREMENTS, USED GPS SATELLITES, TIME, AND VERTICAL OF PRECISION. UNDERLINED SATELLITES PROVIDED REFLECTIONS THAT GO UNDER THE BRIDGE

TIME	SV	TDOP	VDOP
13.29	7 15 16	2.4	1.7
13.44	4 7 16	1.2	0.9
14.05	4 7 16	1.2	0.8
15.36	4 24	1.4	1.0
15.51	4 24	1.9	1.3
16.07	4 10 19 24	1.1	0.8
16.22	4 10 16 19 24	0.9	0.7

lites (marked with a filled circle ●). The number near each GPS satellite trace is the PRN number associated with the satellite. In Table I, the time of the measurements (local time, i.e., central European summer time) is reported and, for each measurement, the specific GPS satellites taken into consideration. The vertical and time dilution of precision (VDOP and TDOP, respectively) are also provided in Table I, showing that despite the small number of GPS satellites, the resulting constellation geometry was reasonably good for sea surface height estimation (values are always below 2.5).

Ground truth information on the tide, sea surface conditions and meteorology was provided by the "Hydro Meteo Centrum Zeeland." The tide and significant wave height are plotted in Fig. 4. During the experiment, the tide raised the water level from −100 to −25 cm below mean sea level in Amsterdam Harbour (Normaal Amsterdams Peil -N.A.P.). The significant wave height was around 1.3–1.4 m.

B. Sea Surface Height Estimation

The processing for both the direct and the reflected signals was done in the same way. A clear replica of each direct GPS signal is generated and up-converted to the IF frequency plus

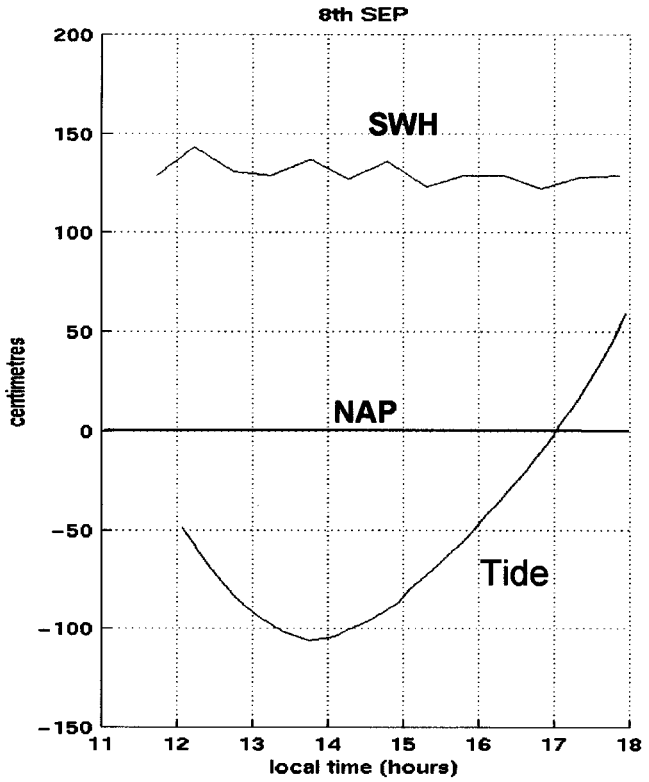

Fig. 4. Tide and significant wave height at the Zeeland bridge on Sept. 8, 1997. Courtesy of the "Hydro Meteo Centrum Zeeland."

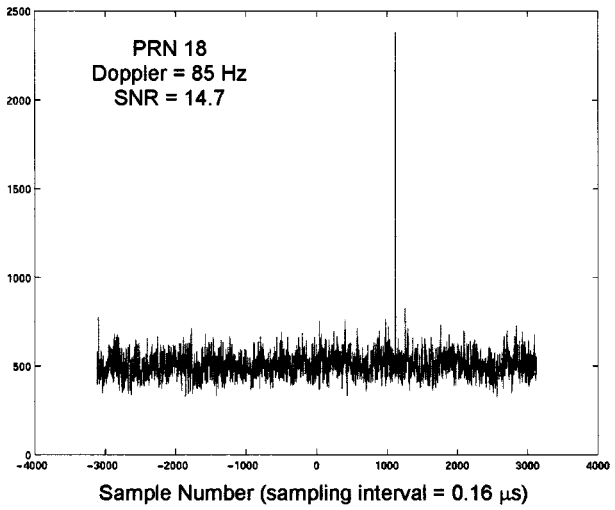

Fig. 5. Typical cross-correlation result between a clean replica of the signal expected from a particular satellite and the received direct (or reflected) signal.

its own Doppler frequency due to GPS satellite motion. The duration of these replica signals is 20 ms, that is, 20 C/A code periods. The Doppler frequency values used are those reported in the rinex files. Each of the replica signals is then cross-correlated with the direct and the reflected signal. The results of such operation are two signals resembling the autocorrelation function of a PRN code: a high triangular-shaped spike in low noise-like signals. An example is presented in Fig. 5.

Each pair of cross-correlation signals (replica-direct signal and replica-reflected signal) is zoomed and interpolated around

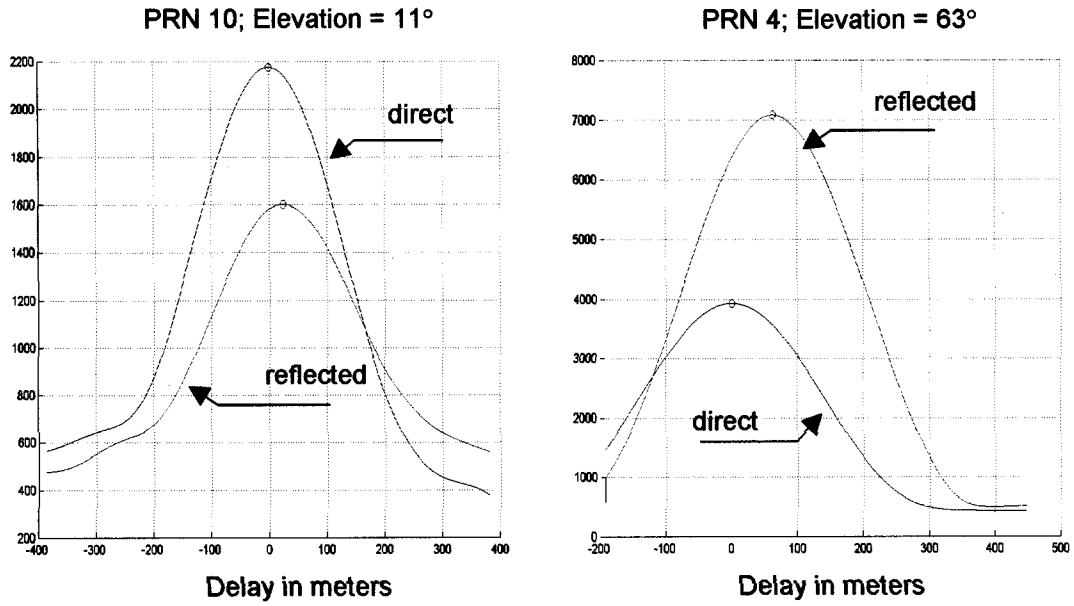

(a) (b)

Fig. 6. Typical cross-correlation result, after interpolation, for direct and reflected signals. The effect of elevation angle in relative delay and amplitude is illustrated for (a) a low elevation and (b) a high elevation GPS satellite. The waveform is symmetric, quite different to the echo shape of typical altimeters, because of the beam-limited condition from the bridge.

the spike using the INTERP function of MATLAB. This function resamples data at a higher rate using low pass interpolation. A typical result of the interpolated cross-correlation functions is shown in Fig. 6. These curves do not look like typical altimeter waveforms indeed. The reason for this is that in this experiment, the footprint is beam-limited and not pulse-limited, mainly due to the small height provided by the bridge (about 18 m) as compared to the C/A-code chip length (300 m). While the iso-delay corresponding to one chip is an ellipse of almost 300 m diameter, the antenna footprint is a circle of only some 25 m (70° beamwidth, or 9 dBic antenna gain, at 18 m height).

Although the hardware set-up was not amplitude-calibrated, the effect of the different gain of the uplooking (2 dBic) and downlooking (9 dBic) antennas can be seen on the amplitude of the cross-correlation functions. This can be understood with the help of Fig. 7 where the glistening area for $\beta_o = 4^\circ$ (area from which most of the reflected power comes from [10]) for elevation angles of 90°, 60°, and 30° has been plotted together with the -3 dB contour of the narrow 9 dBic antenna gain beam. For low elevation satellites, as PRN 10 in Fig. 6(a), the glistening area falls mostly outside the downlooking antenna footprint resulting in a low amplitude reflected signal. For high elevation satellites, as PRN 4 in Fig. 6(b), the glistening area is seen with the higher gain of the downlooking antenna and the reflected signal has a larger amplitude than the direct signal.

To proceed with the estimation of the sea surface height, the peak of the two interpolated cross-correlation functions is determined, and then the delay between them is derived. The delay between the peaks is assumed to be the time lag of the reflected signal with respect to the direct signal. Such an assumption implies that the model of the reflected signal is simply the same model of the direct signal except for a time shift. The justification for this follows. The peak of the cross correlation of the

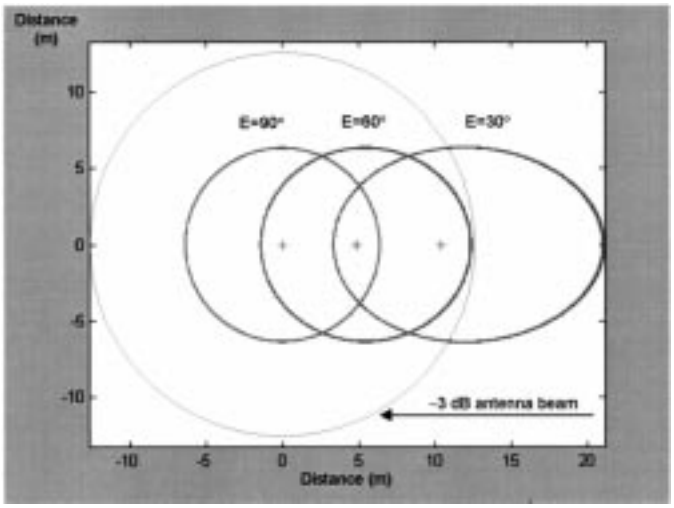

Fig. 7. Glistening area (area which most of the reflected energy comes from) for 90°, 60°, and 30° elevation angles. The -3 dB beam contour of the high gain downlooking antenna (9 dBic) is shown. Low elevation reflected signals are strongly attenuated by the antenna pattern.

reflected signal does not correspond exactly to the delay at the point of specular reflection because a) the surface is rough, not flat, and roughness will introduce an asymmetry in the waveform, and b) the antenna pattern and the free space loss change across the chip-limited footprint. However, the corresponding induced errors are estimated to be smaller than the observation noise, this being the major error source, as discussed next.

In a first approximation the measurement noise in each 20 ms delay observation is estimated to be $\sigma_\tau = 8.4$ m according to

$$\sigma_\tau = \frac{T_c}{\sqrt{2TP_s/N_o}} \tag{5}$$

where

$Tc = 300$ m	C/A code chip length;
$T = 20$ ms	integration time;
$P_s = -160$ dBW	power of the signal for an average elevation;
$N_o = -205$ dBW/Hz	noise power density.

Some 105 of these samples were averaged over a 2.56 s observation window resulting in a further improvement of delay estimation by a factor of 10.2, giving $\sigma'_\tau = 0.82$ m. The measurement noise has to be compared with a surface roughness of about $\sigma_\varsigma = 0.35$ m RMS (SWH $= 1.4$ m), which is smoothed out in 2.56 s by a factor of five (assuming a coherence time of the sea surface of 100 ms) to give, effectively, $\sigma'_\varsigma = 7$ cm RMS. Thus, there is an order of magnitude difference between the measurement noise and the roughness-induced noise.

Concerning the effect of antenna pattern gain and free space loss weighting across the pulse-limited footprint, no numerical computation was carried out since the antenna pattern was not available. However, both weightings (antenna gain and path loss) are rather uniform across delays (refer to Fig. 7), that is, all isodelay ellipses are weighted quite in the same way regardless the delay. The contribution from points of the surface closer to the receiver is amplified by the gain of the antenna and by a shorter free space path. The contribution from points further to the receiver is attenuated by a lower antenna gain and by a longer free space path. Such uniform weighting over delay is likely to introduce a bias smaller than the measurement noise presented above.

Bearing in mind the above limitations of the simple model for the reflected signal and using the geometry of Fig. 1, the relative delay τ between direct and reflected signals can be related to the height of the bridge over the sea surface h, the elevation of the GPS satellite E, and the differential clock bias between the two GPS receivers T_B by

$$c\tau = 2h \sin E + cT_B. \tag{6}$$

The estimated relative delays of the reflected signals show the correct behavior with respect to the elevation angle of the GPS satellites, that is, low elevation satellites have shorter delays than high elevation satellites. This can be verified in Fig. 6, where the delay for PRN 10 at 11° elevation is about half the delay for PRN 4 at 63° elevation angle.

The estimation of the height of the bridge and the clock bias is carried out in two sequential steps: 1) estimation of delays of the reflected signals for all valid GPS satellites and 2) least squares fit to retrieve the two unknowns using (6).

In the first step, the 20 ms cross correlation functions for the direct and reflected signals are computed for each satellite within the visibility mask and the delay between peaks is stored in a measurement vector. As mentioned earlier, the data used are those collected during the second day: 28 recordings of 2.56 s each. From each recording, some 105 values of delay have been derived for the valid satellites using the 20 ms cross correlations. All the delays estimated from data collected within 10 min were averaged as they were considered to be representative of the same sea surface height (within 10 min there were either one or two recordings of 2.56 s available). The resulting averaged delays for all valid satellites are shown in Fig. 8 (with circles "○") together with the theoretical value of delay assuming

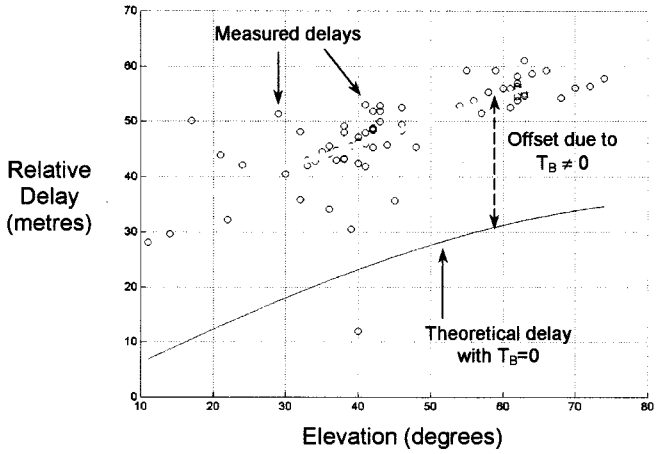

Fig. 8. Measured delays (with circles) compared to theoretical delays, assuming no time bias (solid line) as a function of elevation angle. The offset between the circles and the solid line is due to the differential clock bias between the two GPS receivers.

$T_B = 0$ (solid line) as a function of the elevation angle. The delay offset between the measured circles and the theoretical solid curve is due to the differential clock bias between the GPS receivers. Surface roughness and other unaccounted effects are embedded in these measurements, and so they have inherently an error, but as discussed above, it is estimated to be smaller than the measurement noise itself. A well known result from GPS positioning is also shown in Fig. 8. The dispersion of the measurements at low elevation is higher than at high elevation. As a consequence, high elevation satellites should be preferred for sea surface altimetry than low elevation satellites.

The second step is the estimation of the height of the bridge and the clock bias through a least squares fit using (6) and the averaged delay measurements from the first step. Therefore, the computation of height and clock bias is not performed by fitting a model to a waveform but to a single point, which is the delay between waveform peaks. By grouping together all valid 2.56 s data recordings in each 10 min interval as explained before, seven estimations of the height bridge (sea surface height relative to the bridge) and the clock bias could be carried out. The retrieved height values were then compared against the true values. The true heights were computed using the tide information and the data from the bridge structure, all height values being referred to N.A.P. The seven estimations (broken line) and the true height (smooth line) are shown in Fig. 9. The error for each one of the seven estimations is calculated as the difference between the measured height and the true height. An RMS error is also computed using the seven estimations yielding 3.3 m, which is roughly 1% of the C/A-code chip (300 m). The RMS height error gives an indication of the goodness of the fit of the data to (6).

The final result of the estimated height is perhaps the best proof of the overall consistency of the assumptions made above regarding surface roughness, antenna pattern and free space loss. The average of the seven measurements in Fig. 9 is 19.3 m, while the true average height of the bridge at those seven points is 18.0 m. The average difference is then 1.3 m, of which $\sigma_\tau \mathrm{VDOP}/\sqrt{7} = 0.82 \times 1.0/\sqrt{7} = 0.3$ m are due to the smoothed measurement noise. Therefore, the measured

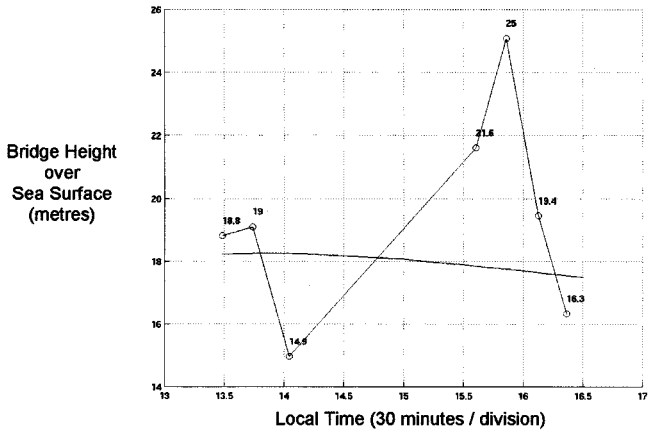

Fig. 9. Estimated height of the bridge over the sea surface. The smooth solid line represents the true value obtained from the NAP heights of bridge and tide. The RMS across the seven estimations is 3.3 m, that is, 1% of the C/A-code chip using an observation time of about 5 s maximum.

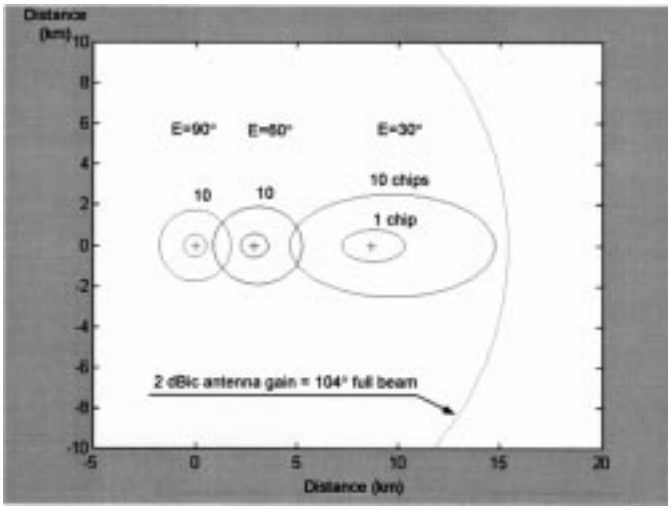

Fig. 10. Iso-delay curves for 1 and 10 P-code chips and for 90°, 60°, and 30° elevation angles in the case of a 5 km altitude aircraft. The −3 dB beam contour of a low-gain (2-dBic) downlooking antenna is shown. Even low elevation reflected signals (such as 30°) are observed over at least ten-chip delays (many more for higher elevations).

upper limit of the height biases induced by surface roughness, antenna, and free space loss weighting is 1 m, which is in the order of the measurement noise. Finally, it is worth noting that since these effects depend on the elevation of the satellite, most of the error caused by them must appear as a height error rather than as a clock bias error, because it is the term involving the height that multiplies the sinus of the elevation angle in (6).

C. Lessons Learned and Future Work

From the 1997 Zeeland Bridge experiment, we have learned 1) the potential accuracy using the ten times wider bandwidth P-code is about 30 cm, provided a more sophisticated model for the reflected signal is used to take care of possible systematic errors on the more precise observations, 2) a more precise height estimation can be achieved if the effect of surface roughness, antenna pattern, and free space loss are accounted for, since the waveform condition from the bridge is beam-limited, and 3) larger heights and a wider downlooking antenna beamwidth are required if a long waveform of many chips is to be observed (from the bridge the waveform was less than 1 C/A code chip). To investigate the first two points, we shall repeat the bridge experiment by the end of 1999 using L1/L2 P-code receivers with carefully calibrated antennas. As for the third point, the only solution is to go for an aircraft test. Assuming an altitude of 5 km, suitable waveforms should be measured. This is illustrated in Fig. 10, where the iso-delay lines for 1 and 10 P-code chips and elevation angles of 90°, 60°, and 30° have been plotted as seen from 5 km height, together with the −3 dB contour of a wide 2-dBic antenna gain beam. It is clear that even for the lower elevation of 30° at least ten chips of the waveform can be observed and many more for higher elevation angles. This provides essentially a pulse-limited condition, as desired. The difficult part for sea surface altimetry from an aircraft comes from all the necessary corrections in the positioning of both the uplooking and the downlooking antenna. However, this should be possible applying kinematic techniques if a third reference receiver is used on the ground.

As for the future of the PARIS concept, one has to look into the trends of the global navigation satellite systems (GNSSs). GNSS systems will be designed and built in the future taking into account safety-of-life civilian applications such as civil aviation. Civil aviation is a strong driver in the modernization of the U.S. GPS system as well as in the definition of the future European Galileo satellite navigation system. In general, GNSS systems (GPS, GLONASS, Galileo) will evolve in the future providing increased capabilities: more satellites, higher power levels, and more carriers frequencies with higher chip rates. But the most important feature of GNSS systems is certainly the continuity of service for decades. The PARIS concept will undoubtedly benefit from these enhancements: capability of even higher spatial-temporal sampling, smaller and simpler antennas needed in the satellite instrument, better sea surface height accuracy, and long term continuity of ocean observations.

V. Conclusions

This paper has briefly reviewed the PARIS concept on the use of GNSS ocean reflected signals as it originated within ESA in 1993 as a solution to the problem of mesoscale ocean altimetry. An original experiment to demonstrate the capability of using GPS reflected signals for sea surface height determination has been presented. The experiment was performed over the Zeeland Bridge in The Netherlands and the measurement constraints have been explained, namely an operation in beam-limited conditions using only C/A-code GPS signals and data processing based on a simple signal reflection model. Yet the final RMS error (RMSE) of the estimated sea surface height with respect to the true value is 3.3 m, that is, about 1% of the chip length using an observation time of about 5 s maximum. The estimated potential accuracy using the ten times wider bandwidth P-code is about 30 cm, provided a more sophisticated model for the reflected signal is used to take care of possible systematic errors on the more precise observations. The future of the PARIS concept for ocean altimetry is promising based on the enhanced capabilities that GNSS systems will offer in the coming decades.

APPENDIX
REFLECTED SIGNAL WAVEFORM EQUATION

Inserting (1) and (2) into (3) gives

$$R_{x_d x_r}(\tau;t) = \int F(\mathbf{P})\sqrt{\sigma(\mathbf{P})} \cdot \langle p\,[t - r_d(t)/c]\; p\,[t - \tau - r(\mathbf{P}, t-\tau)/c] \cdot e^{-j2\pi f_c[\tau - r_d(t)/c + r(\mathbf{P}, t-\tau)/c]} \rangle\, dA(\mathbf{P}) \tag{7}$$

where the ionospheric effect for the case of the bridge experiment has been neglected.

The time argument of the second C/A-code in (7) can then be written as

$$\begin{aligned} -\tau - r(\mathbf{P}, t-\tau)/c &= -\tau - r(\mathbf{P}, t)/c + \tau\,\dot{r}(\mathbf{P}, t)/c \\ &= -\tau\,[1 - \dot{r}(\mathbf{P}, t)/c] - r(\mathbf{P}, t)/c \end{aligned} \tag{8}$$

where

$$\dot{r}(\mathbf{P}, t)/c \ll 1 \tag{9}$$

The phase argument in (7) can be expanded as follows:

$$\begin{aligned} &\tau - r_d(t)/c + r(\mathbf{P}, t-\tau)/c \\ &\quad = \tau - r_d(t_o)/c - (t - t_o)\;\dot{r}_d(t_o) \\ &\qquad /c + r(\mathbf{P}, t_o)/c + (t - \tau - t_o)\dot{r}(\mathbf{P}t_o)/c \end{aligned} \tag{10}$$

The case of interest happens when the instrumental delay τ compensates the path difference between the direct and the reflected signal at t_o and when $\tau \ll t - t_o$, in which case (10) becomes

$$\begin{aligned} &\tau - r_d(t)/c + r(\mathbf{P}, t-\tau)/c \\ &\quad = (t - t_o)\;\left[\dot{r}(\mathbf{P}, t_o) - \dot{r}_d(t_o)/c\right]. \end{aligned} \tag{11}$$

Taking (8) and (11) into (7) gives

$$R_{x_d x_r}(\tau;t) = \int F(\mathbf{P})\sqrt{\sigma(\mathbf{P})} \cdot \langle p\,[t - r_d(t)/c]\; p\,[t - \tau - r(\mathbf{P}, t)/c] \cdot e^{-j2\pi(t - t_o) f_d(\mathbf{P}, t_o)} \rangle\, dA(\mathbf{P}). \tag{12}$$

The average inside the integral is estimated integrating over a multiple number of the C/A-codes. During the basic integration time $T_o = 1$ ms, the exponential in (12) can be considered constant for the doppler frequency of the reflected signal relative to the direct signal in the bridge experiment is very small. Therefore

$$\begin{aligned} &\frac{1}{T_o}\int_{T_o} p\,[t - r_d(t)/c]\; p\,[t - \tau - r(\mathbf{P}, t)/c] \\ &\qquad \cdot e^{-j2\pi(t - t_o) f_d(\mathbf{P}, t_o)}\, dt \\ &\quad = R_p\,[\tau - r_d(\mathbf{P}, t)/c]\, e^{-j2\pi(t - t_o) f_d(\mathbf{P}t_o)}. \end{aligned} \tag{13}$$

When several periods of 1 ms are accumulated over an integration time $T = NT_o$ for which the time argument of R_p does not change appreciably then

$$\begin{aligned} &\frac{1}{N}\sum_{i=0}^{N-1} R_p\,[\tau - r_d(\mathbf{P}, t_i)/c]\, e^{-j2\pi(t_i - t_o) f_d(\mathbf{P}, t_o)} \\ &\quad = R_p\,[\tau - r_d(\mathbf{P}, t_o)/c]\,\frac{1}{N}\sum_{i=0}^{N-1} e^{-j2\pi(t_i - t_o) f_d(\mathbf{P}, t_o)} \end{aligned} \tag{14}$$

which, when inserted in (12) gives (4).

ACKNOWLEDGMENT

The authors would like to acknowledge the support received from M. Lopriore, ESA, and the work performed by Engineers Dr. C. Martín-Rodriguez and T. Feliu-Bassols in helping with the cumbersome equations describing the PARIS concept.

REFERENCES

[1] *Proc. Consultative Meeting on Imaging Altimeter Requirements and Techniques*, Mullard Space Sci. Lab., June 1990.

[2] Alenia, "Final report for the constellation of pulse limited nadir looking radar altimeters,", IAB/FR/ALS/001, ESTEC Contract 9370/91, 1992.

[3] "*Proc. de mesures altimétriques aériennes ou spatiales, notamment destiné à l'altimétrie des océans, et dispositif mettant en* œuvre un tel procédé, Demande de Brevet d'Invention de l'Agence Spatiale Europeenne,", Tech. Rep. 93 13 192.

[4] M. Martín-Neira, "A passive reflectometry and interferometry system (PARIS): Application to ocean altimetry," *ESA J.*, vol. 17, pp. 331–355, Dec. 1993.

[5] G. Picardi, R. Seu, S. Sorge, and M. Martín-Neira, "Bistatic model of ocean scattering," *Trans. Antennas Propagat.*, vol. 46, pp. 1531–1541, Oct. 1998.

[6] J. C. Auber and A. Bibaut, "Characterization of multipath on land and sea at GPS frequencies," in *Proc. Inst. Navigation ION GPS-94 Conf.: Part 2*, Paris, France, Sept. 1994, pp. 1155–1171.

[7] Steve Lowe, "LEO detection of an ocean-reflected GPS signal," in *Proc. GPS Surface Reflections Workshop at Goddard Space Flight Center*, Jet Propulsion Lab., Pasadena, CA, July 1998.

[8] ENVISAT, *The Altimetry Report: Science and Applications*. Noordwijk, The Netherlands: Eur. Space Agency, ch. 4, pp. 41–72.

[9] M. Caparrini, "Using reflected GNSS signals to estimate surface features over wide ocean areas,", ESTEC Working Paper 2003, Dec. 1998.

[10] P. Beckmann and A. Spizzichino, *The Scattering of Electromagnetic Waves from Rough Surfaces*. Norwood, MA: Artech House, ch. 5, pp. 70–98.

Manuel Martín-Neira received the M.S. and Ph.D. degrees in telecommunication engineering from the School of Telecommunication Engineering, Polytechnic University of Catalonia (UPC), Catalonia, Spain, in 1986 and 1996, respectively.

He was awarded a Fellowship to work on radiometry at the European Space Research and Technology Center (ESTEC), Noordwijk, The Netherlands, in 1988. From 1989 to 1992, he joined GMV, a Spanish firm, where he was responsible for several projects for the European Space Agency (ESA) related to GPS spacecraft navigation with applications to precise landing and attitude determination. He has been with ESA since 1992, where he is in charge of the radiometer activities within the Payload Systems Division (D/TOS). During this period, he has also developed new concepts for constellations of small satellites for Earth observation. In particular, he holds a patent on the PARIS concept.

Marco Caparrini received the Laurea in electronic engineering (spec. remote sensing) in 1995 from the University of Rome "La Sapienza," Rome, Italy. He is currently pursuing the Ph.D. degree on model-based remote sensing image analysis for snow segmentation in mountainous areas with the Swiss Federal Institute of Technology (ETH), Zürich.

In 1997, he joined the European Space Agency (ESA), European Space Research and Technology Center (ESTEC), Noordwijk, The Netherlands, in the Electrical Engineering Department, working mainly on GNSS signals reflection on Earth surface for Earth Observation purposes.

J. Font-Rossello received the degree in telecommunication engineering in 1995 from the School of Telecommunication Engineering, Polytechnic University of Catalonia (UPC), Catalonia, Spain.

In 1996, he was awarded a Fellowship from the Spanish Ministerio de Industria to work on communications at the European Space Operations Center (ESOC) and one year later on microwave instruments for Earth Observation at the European Space Research and Technology Center (ESTEC). In 1997, he developed techniques for microwave radiometry in alias conditions and participated in the theoretical development and realization of the Zeeland bridge experiments. He is currently teaching in Mallorca Island, Spain.

Stephane Lannelongue received the M.Sc. engineer degree in electronics and electricity with a specialization in signal processing from the Ecole Nationale Suprieure d'Ingnieurs Electriciens de Grenoble (ENSIEG), France, in 1996.

Since 1997, he has been working as a Radio Navigation Engineer in the research center of the European Space Research and Technology Center (ESTEC), European Space Agency, Noordwijk, The Netherlands. During this time, he has been involved in several activities related to navigation such as the development of fast acquisition techniques for GPS receivers, GNSS validation for civil aviation, and the localization of jammers for radio-navigation application.

Circe Serra Vallmitjana received the M.S. degree from the Polytechnic University of Catalonia (UPC), Catalonia, Spain, in 1998.

During the summer of 1997 in 1998, she was with the Metropolitan Transports of Barcelona (TMB), Barcelona, Spain, and the Astrophysics Institute of the Canary Islands (IAC). She is currently a Telecommunications Engineer, specializing in communications. Since December 1998, she has been with the European Space Research and Technology Center (ESTEC), Noordwijk, The Netherlands, in the Payload, Equipment and Technology Section. She is currently working in the domain of mesoscale ocean altimetry using GNSS reflected signals.